Effect of the Z Mutation on the Physical and Inhibitory Properties of α_1-Antitrypsin†

David A. Lomas,* Dyfed Ll. Evans, Stuart R. Stone, Wun-Shaing W. Chang, and Robin W. Carrell

Department of Haematology, University of Cambridge, MRC Centre, Hills Road, Cambridge CB2 2QH, U.K.

Received August 13, 1992; Revised Manuscript Received November 2, 1992

ABSTRACT: A major feature of the structure of α_1-antitrypsin is a five-stranded A-sheet into which the reactive center loop inserts after cleavage. We describe here the effect of the Z mutation (^{342}Glu to Lys) at the head of the fifth strand of the A-sheet on the mobility of the reactive center loop and hence on the physical properties of the antitrypsin molecule. The mutant Z but not the normal M antitrypsin spontaneously polymerizes at 37 °C by a mechanism involving the insertion of the reactive center loop of one molecule into the A-sheet of a second. It is demonstrated that Z antitrypsin polymerized after incubation with 1.0 M guanidinium chloride at 37 °C at the same rate as M antitrypsin. Reducing the temperature to 4 °C favored the formation of the L-state in M antitrypsin in which the loop is stably incorporated into the A-sheet, but resulted in loop–sheet polymerization in Z antitrypsin. Z, like M antitrypsin, undergoes the *S* to *R* transition, but we show that the accompanying change in thermal stability results from loop–sheet polymerization (*S*) which can be prevented by the insertion of the cleaved strand of the reactive center loop into the A-sheet (*R*). Z antitrypsin has a reduced association rate constant with neutrophil elastase [$(5.3 \pm 0.06) \times 10^7$ and $(1.2 \pm 0.02) \times 10^7$ M^{-1} s^{-1} for M and Z, respectively], but both M and Z antitrypsin had K_i values of less than 5 pM. Residues P_9–P_{10} of the reactive center loop can be enzymatically cleaved in native M antitrypsin, but these residues are inaccessible in the binary complex of M antitrypsin with a reactive center loop peptide and in native as well as binary complexed Z antitrypsin. This together with the CD spectrum of Z antitrypsin suggests a rearrangement of the loop with opening of the A-sheet to allow spontaneous intermolecular loop–sheet polymerization.

α_1-Antitrypsin is the archetypal member of the serine proteinase inhibitor (serpin) superfamily. Members of this family each have a unique inhibitory specificity but share a similar molecular structure (Huber & Carrell, 1989). The major feature of this structure is the A-sheet, a five-stranded β-pleated sheet into which the reactive center loop inserts following cleavage. The structure of the cleaved form is known (Loebermann et al., 1984; Baumann et al., 1991), but that of the native inhibitor has yet to be determined. The only intact model is that of the noninhibitor ovalbumin (Stein et al., 1990) in which the reactive center loop is in the form of an extended three-turn helix. As such this is an unsatisfactory conformation for inhibition, and predictably the helix will require opening in the inhibitory serpins by the partial insertion of its N-terminal stalk into the A-sheet (Stein et al., 1991).

It is now apparent that the serpin reactive center loop is mobile and able to adopt varying conformations (Carrell et al., 1991; Mottonen et al., 1992). For example, under mild denaturing conditions at 4 °C the reactive center loop of antitrypsin can be locked into the A-sheet, forming a thermostable, inactive protein, the L-state (Carrell et al., 1991). In contrast, if the temperature is elevated to 37 °C, these same denaturing conditions favor the insertion of the reactive center loop of one antitrypsin molecule into the A-sheet of a second, so-called, loop–sheet polymerization (Evans, 1991; Mast et al., 1992; Lomas et al., 1992).

Most northern Europeans have only the normal M form of antitrypsin, but some 4% are heterozygotes for the Z deficiency variant (Laurell & Eriksson, 1963). This variant results in a blockage in the final stage of processing in the liver such that in the homozygote only 15% of the protein is secreted into the circulation. The Z mutation of antitrypsin, ^{342}Glu to Lys (Jeppsson, 1976), is likely to affect the mobility of the reactive center loop as it forms its hinge at the head of the fifth strand of the A-sheet in close proximity to the partially inserted loop. The perturbation at this critical hinge region is supported by the demonstration that the Z mutant undergoes spontaneous loop–sheet polymerization in vivo (Lomas et al., 1992). This polymerization provides an explanation for the retention of antitrypsin within the rough endoplasmic reticulum of hepatic cells in Z homozygotes and hence the associated plasma deficiency.

We report here studies to determine the effect of the Z mutation on the mobility of the reactive center loop and hence the inhibitory activity of the molecule. These studies include the induced formation of the L-state and loop–sheet polymers, the accessibility of the loop to proteolytic cleavage, changes in circular dichroic spectra, the *S* to *R* transition, and the kinetics and stability of complex formation with proteinases.

EXPERIMENTAL PROCEDURES

Materials. Human neutrophil elastase was from Drs. C. Ward and S. Afford, Lung Immunobiochemical Research Laboratory, General Hospital, Birmingham, U.K. Bovine α-chymotrypsin, neurotensin, methoxysuccinyl-L-alanyl-L-alanyl-prolyl-L-valyl-*p*-nitroanilide and succinyl-L-alanyl-L-alanyl-prolyl-L-phenylalanyl-*p*-nitroanilide were from Sigma Chemical Co., Dorset, U.K. Papaya proteinase IV was from Calbiochem, Nottingham, U.K.

Purification of Z Antitrypsin. M and Z antitrypsin were purified from the plasma of M and Z homozygotes, respectively. All the steps in the procedure were performed at 4 °C.

† This work was supported by the Medical Research Council and the Wellcome Trust. D.A.L. is an MRC Training Fellow, and D.Ll.E. is an Elmore Fellow.

* To whom correspondence should be addressed.

0006-2960/93/0432-500$04.00/0 © 1993 American Chemical Society

Eighty-five milliliters of Z plasma (antitrypsin concentration 0.2 mg/mL) and 400 mL of M plasma were diluted with equal volumes of saturated ammonium sulfate containing 0.28% v/v β-mercaptoethanol. The mixture was stirred for 15 min and the precipitate removed by centrifuging at 1500*g* for 20 min. The supernatant was retained and the precipitate washed with 50% w/v ammonium sulfate and 0.14% v/v β-mercaptoethanol. The washed precipitate was also centrifuged at 1500*g* for 20 min, and the supernatants were pooled. Solid ammonium sulfate was then added with stirring to 70% w/v, the pH was adjusted to 6.0 with sulfuric acid, and the mixture was gently stirred for a further 30 min prior to centrifugation at 1500*g* for 45 min. The supernatant was then discarded and the precipitate dissolved in a minimum volume of 0.1 M Tris and 5 mM EDTA, pH 8.0. This solution was dialyzed against 5 L of 5 mM EDTA, pH 8.0, with two changes and then against 5 L of 0.1 M Tris and 5 mM EDTA, pH 8.0.

The solution was then applied to a glutathione–Sepharose column (Laurell et al., 1975) which had been prepared by washing on a Buchner funnel with 500 mL of deionized 8 M urea and 0.17% v/v β-mercaptoethanol; 250 mL of 0.1 M Tris, 5 mM EDTA, 1.0 M sodium chloride, and 0.17% v/v β-mercaptoethanol, pH 8.0; 250 mL of 0.1 M sodium acetate; 5 mM EDTA, 1.0 M sodium chloride, and 0.17% v/v β-mercaptoethanol, pH 4.0; 250 mL of 0.1 M Tris, 5 mM EDTA, 1.0 M sodium chloride, and 0.17% v/v β-mercaptoethanol, pH 8.0; 250 mL of 0.1 M sodium acetate, 5 mM EDTA, 1.0 M sodium chloride, and 0.17% v/v β-mercaptoethanol, pH 4.0, and equilibrating with 0.1 M Tris and 5 mM EDTA, pH 8.0 (equilibration buffer). The column (32 × 2.5 cm) was packed and run at a flow rate of 88 mL/hr, charged with 100 mL of 5,5′-dithiobis(2-nitrobenzoic acid) (DTNB) solution (0.1% w/v DTNB, 0.1 M Tris, 5 mM EDTA, pH 8.0), and washed with equilibration buffer until the base line returned to zero. The sample was loaded onto the column and washed with 100 mL of 0.5 M sodium chloride, 0.1 M Tris, and 5 mM EDTA, pH 8.0, and then with equilibration buffer until the base line returned to zero. Bound protein was eluted from the column with 30 mL of DTNB/TNB solution (30 mg of DTNB and 6 mg of dithiothreitol in 0.1 M Tris and 5 mM EDTA, pH 8.0) and the column washed with equilibration buffer.

Fractions containing α_1-antitrypsin were identified by rocket immunoelectrophoresis (Weeke, 1973). These were pooled and then concentrated and reduced to remove TNB by dialyzing against 0.1 M Tris, 5 mM EDTA, and 0.1% v/v β-mercaptoethanol, pH 8.6, in an Amicon concentrating cell. The flow-through also contained antitrypsin, and therefore the column was regenerated and the protein passed over it for a second time. The eluates from both passes were pooled, and the resulting solution was loaded onto a Q-Sepharose column (36.5 × 1.6 cm) which had been washed with 2.5 M sodium chloride, 0.1 M Tris, and 5 mM EDTA, pH 8.6, and equilibrated with 0.1 M Tris, and 5 mM EDTA, pH 8.6. The column was washed with the same buffer and the α_1-antitrypsin eluted with a 0–0.4 M sodium chloride gradient in 0.1 M Tris and 5 mM EDTA, pH 8.6 (total volume 1 L). The fractions containing α_1-antitrypsin were identified by rocket immunoelectrophoresis, pooled, and concentrated to 1 mg/mL in 50 mM Tris, 50 mM KCl and 0.1% v/v β-mercaptoethanol, pH 7.4, storage buffer. Total protein was determined from the OD_{280} (Travis & Johnson, 1981) and purity assessed by 10–20% w/v sodium dodecyl sulfate–polyacrylamide gel electrophoresis (SDS–PAGE) (Laemmli, 1970) and amino-terminal sequencing following transfer onto Problot membrane (Towbin et al., 1979).

Scheme I

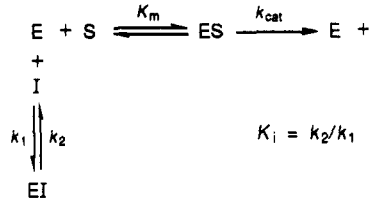

Active Site Titration of Antitrypsin. Active site titration was performed by incubating bovine α-chymotrypsin of known active site (Kezdy & Kaiser, 1970) with increasing concentrations of antitrypsin and 0.03 M sodium phosphate, 0.16 M NaCl, and 0.1% w/v PEG 4000, pH 7.4, reaction buffer in a volume of 100 μL. The mixture was incubated for 10 min at room temperature and the residual proteolytic activity determined by adding reaction buffer containing the substrate succinyl-L-alanyl-L-alanyl-prolyl-L-phenylanalyl-*p*-nitroanilide (Suc-Ala-Ala-Pro-Phe-pNA; final concentration 0.16 mM) to a final volume of 1 mL and observing the change in OD_{405} for 3 min. Active site values were obtained by plotting residual proteolytic activity against the amount of inhibitor and extrapolating to the *x*-intercept (Beatty et al., 1980). The active site value of neutrophil elastase was determined by the same method using antitrypsin of known activity and the substrate methoxysuccinyl-L-alanyl-L-alanyl-prolyl-L-valyl-*p*-nitroanilide (MeO-Suc-Ala-Ala-Pro-Val-p-NA).

Determination of Kinetic Parameters for the Association of Antitrypsin with Neutrophil Elastase and Bovine α-Chymotrypsin. Kinetic parameters for the interaction of M and Z antitrypsin with human neutrophil elastase and bovine α-chymotrypsin were determined in the presence of substrate by analyzing the progress curves for the formation of *p*-nitroaniline. The assays were performed at 37 °C in 0.03 M sodium phosphate, 0.16 M NaCl, and 0.1% w/v PEG 4000, pH 7.4, reaction buffer with all neutrophil elastase reactions containing 0.1% v/v Triton X-100. The substrates MeO-Suc-Ala-Ala-Pro-Val-pNA and Suc-Ala-Ala-Pro-Phe-pNA were present at a concentration of 400 μM for elastase and chymotrypsin, respectively. A typical progress curve experiment consisted of 6 assays (1 zero and 5 nonzero concentrations of inhibitor). The assays were started by the addition of enzyme, the final concentrations of elastase and chymotrypsin being 56 and 100 pM, respectively. The inhibition of the enzymes (E) by antitrypsin (I) can be described by Scheme I, where S is the substrate and P is *p*-nitroaniline. The progress curve data were fitted by nonlinear regression to the equation describing this mechanism of slow, tight-binding inhibition (Stone & Hofsteenge, 1986; Morrison & Walsh, 1987). For assays with elastase, the value of the dissociation rate constant (k_2) approached zero; that is, K_i was very small and the inhibition appeared irreversible. For analysis of these data, k_2 was set to zero. The analyses yield values for the apparent association rate constant (k_1') and the apparent dissociation constant (K_i'). These values were corrected for the concentration of substrate using the following equations to yield the true values of the parameters:

$$K_i = K_i'/(1 + [S]/K_m)$$

$$k_1 = k_1'(1 + [S]/K_m)$$

The values of the Michaelis constants (K_m) required in these calculations were determined to be 0.1 ± 0.01 mM for MeO-

Succ-Ala-Ala-Pro-Val-pNA with elastase and 0.087 ± 0.007 mM for Succ-Ala-Ala-Pro-Phe-pNA with chymotrypsin.

Isoelectric Focusing. Isoelectric focusing was performed on a 5% polyacrylamide gel with a pH gradient of 3.5–10 according to the method of Monte et al. (1976). All samples were loaded at the cathode and following focusing were visualized by staining with 0.2% bromophenol blue in 45% (v/v) ethanol, 5% (v/v) acetic acid, and 50% (v/v) water and destaining with 45% (v/v) ethanol, 5% (v/v) acetic acid, and 50% (v/v) water.

Polymerization of M and Z Antitrypsin. Polymerization was induced by incubating the antitrypsin at a range of protein concentrations and temperatures in the storage buffer. The percentage polymer was determined by sequential gel filtration high-performance liquid chromatography (HPLC) on a molecular weight calibrated TSK-2000SW column in 20 mM sodium phosphate and 50 mM NaCl, pH 7.6 (Lomas et al., 1992). Calibration was performed using IgG (150 kDa), C1 inhibitor (115 kDa), bovine serum albumin (66 kDa), and ovalbumin (45 kDa) standards; native antitrypsin was eluted with a predicted molecular weight of 52 kDa. The ratio of the polymerized peak (molecular mass >200 kDa) to the native peak was taken as the percentage of polymerized material.

Binary Complex Formation. The binary complex of M or Z antitrypsin with the antithrombin III-reactive center loop peptide BC13 (Ac-Ser-Glu-Ala-Ala-Ala-Ser-Thr-Ala-Val-Val-Ise-Ala-Gly-OH) was formed by incubating antitrypsin (1 mg/mL) in the storage buffer with 100-fold molar excess of the peptide at 37 °C for 24 h (Schulze et al., 1990). Binary complex formation was confirmed by native PAGE, thermostability, and circular dichroic spectra (Carrell et al., 1991). BC13 was used as it forms binary complexes as readily with antitrypsin as antithrombin (k_{obs} for both reactions = $8 \times 10^{-2}\ M^{-1}\ s^{-1}$). Furthermore, previous studies have shown that an excess of this peptide does not interfere with reactive loop cleavage by papaya proteinase IV.

Circular Dichroism. Circular dichroism (CD) was performed in 20 mM sodium phosphate and 30 mM NaCl, pH 7.8, at 30 °C in a Jobin-Yvon Dichrographe VI instrument. The mean residue ellipticity $[\theta]_{MRW}$ was determined from a mean residue weight of 134, the spectra shown being the average of 18 readings taken on two separate occasions. Spectra in the near-UV range (250–310 nm) were determined with a 1-cm path length cell while those in the far-UV range (200–250 nm) were determined with a 0.1-cm path length cell. Thermal denaturation of M antitrypsin was determined by measuring the relative change in ellipticity at 222 nm of 0.2 mg/mL samples heated for 3 h at increasing temperatures compared to an unheated control.

Heat Stability Assays. M and Z antitrypsin were cleaved at the reactive center loop by incubating with *Staphylococcus aureus* V8 proteinase for 2 h at 37 °C. Complete cleavage was comfirmed by 10–20% SDS–PAGE. The cleaved and native antitrypsin (0.2 mg/mL) in 50% v/v 75 mM Tris, 75 mM glycine, and 75 mM NaH_2PO_4, pH 7.5, were then heated at constant temperatures between 30 and 100 °C for 2 h. The solutions were rapidly cooled on ice, centrifuged, and filtered through a 0.22 μM membrane, and the residual protein concentration was determined by rocket immunoelectrophoresis.

Cleavage of the Reactive Center Loop with Papaya Proteinase IV. M and Z antitrypsin (5 μg) were cleaved with papaya proteinase IV for 2 h at 37 °C in 50% v/v incubation buffer (30 mM potassium phosphate, 30 mM, NaCl, pH 7.0). The cleavage products were assessed by 10–20% SDS–PAGE, and the site of cleavage was determined by isolating the cleaved fragment on a reverse-phase HPLC column (Evans et al., 1991) followed by amino-terminal sequencing.

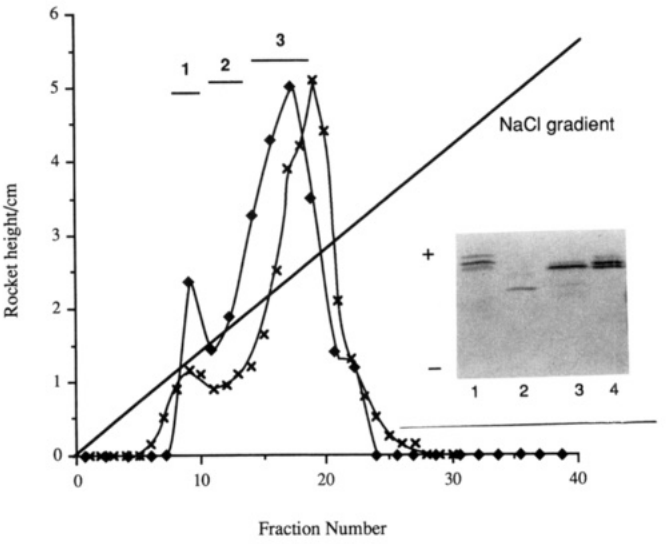

FIGURE 1: Comparison of the profile of M (×) and Z (♦) antitrypsin eluted by a 0–0.3 M NaCl gradient from the Q-Sepharose anion-exchange column. Elution was monitored by rocket immunoelectrophoresis. The M elution profile is that of synovial fluid from an M homozygote in order to allow comparison of amino-terminally cleaved (first peak) with intact (subsequent peaks) material. Z antitrypsin was divided into 3 fractions as illustrated. The inset is the isoelectric focusing pattern of M and Z antitrypsin. Lane 1, M antitrypsin; lane 2, Z antitrypsin fraction 1; lane 3, Z antitrypsin fraction 2; lane 4, Z antitrypsin fraction 3. All lanes were loaded with 15 μg of protein. Lanes 1, 3, and 4 contain amino-terminally intact antitrypsin whereas the protein in lane 2 has 5 residues cleaved from the amino terminus.

RESULTS

Antitrypsin Purification. M and Z antitrypsin had similar elution profiles from the Q-Sepharose column, but as expected Z antitrypsin eluted from the column at a slightly lower salt concentration than M antitrypsin (Figure 1). Interestingly, the large quantities of plasma M antitrypsin resulted in the displacement of other proteins from glutathione–Sepharose, and so virtually pure protein was eluted at this stage of the purification. This was not the case for Z antitrypsin which was further separated from contaminants on a Q-Sepharose column. The elution profile from this column allowed Z antitrypsin to be divided into 3 fractions (Figure 1), each of which was characterized separately.

Each fraction was shown to be pure by SDS–PAGE with specific activities of 30%, 41%, and 75% for fractions 1, 2, and 3, respectively, compared with 78% for M antitrypsin. Fraction 1 showed a cathodal shift on isoelectric focusing (Figure 1, inset, lane 2) shown by sequencing analysis to be due to the cleavage of five amino acids including two negatively charged residues from the amino terminus (^{6}DAAQK–). Amino-terminal sequencing of fractions 2 and 3 and M antitrypsin revealed an intact amino terminus (^{1}EDPQG–); none of the fractions (1, 2, 3, or M) had active site cleavage to account for their reduced specific activity. HPLC gel filtration of each fraction revealed 70% and 60% high molecular mass material (>200 kDa) respectively in fractions 1 and 2 but no such material in fraction 3 or in M antitrypsin. Fraction 3 and M antitrypsin were used in all further experiments.

Effect of Z Loop Sheet Polymerization on Inhibitory Activity. Z and M antitrypsins (2 mg/mL) were incubated at 37 °C and their inhibitory activities assessed against bovine α-chymotrypsin. As Z antitrypsin polymerized, the protein

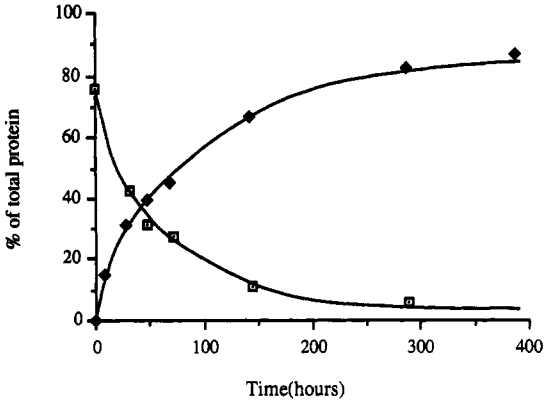

FIGURE 2: Effect of loop–sheet polymerization (♦) on the specific activity (⊡) of Z antitrypsin. Z antitrypsin (2 mg/mL) was incubated at 37 °C and inhibitory activity determined against bovine α-chymotrypsin. The percentage polymerization at each time point was assessed by HPLC gel filtration using 10 μg of protein. M antitrypsin did not polymerize or lose inhibitory activity when incubated under the same conditions.

lost inhibitory activity (Figure 2). There was no loss of inhibitory activity of M antitrypsin which did not spontaneously loop–sheet polymerize under these conditions.

Effect of Concentration and Temperature on the Polymerization of M Antitrypsin. As with Z antitrypsin (Lomas et al., 1992) the spontaneous polymerization of M antitrypsin was dependent upon both temperature (Figure 3a) and protein concentration (Figure 3b). The effect of protein concentration was assessed at 65 °C as incubation of relatively dilute solutions at lower temperatures results in much slower rates of polymerization. Furthermore, loop–sheet polymerization without accompanying denaturation and aggregation was apparent at temperatures up to 85 °C for M antitrypsin. This was confirmed by measuring the relative change in ellipticity at 222 nm as compared to an unheated sample after incubating the protein (0.2 mg/mL) for 3 h at a range of temperatures (Figure 3c). The ellipticity increases between 50 and 60 °C, indicating increased helical packing as a result of loop–sheet polymerization, and then falls again at 85 °C, indicating protein denaturation.

Polymerization of M and Z Antitrypsin with 1.0 M Guanidinium Chloride. M and Z antitrypsin (final concentration 1 mg/mL) were incubated at 37 °C in the presence of 1 M guanidinium chloride. The rates of polymerization were similar, with 69% and 61% of M and Z antitrypsin, respectively, reaching the polymerized form. Polymerization of both M and Z antitrypsins was blocked by binary complex formation with the peptide BC13 but was unaffected by an irrelevant peptide neurotensin (Glu-Leu-Tyr-Glu-Asn-Lys-Pro-Arg-Arg-Pro-Tyr-Ile-Leu) which does not form a binary complex with either protein.

Formation of Latent (L) Form Antitrypsin. Antitrypsin (1 mg/mL) was incubated for 12 h at 4 °C with increasing concentrations of guanidinium chloride as described previously (Carrell et al., 1991) and then diluted 20-fold and the inhibitory activity assessed against bovine α-chymotrypsin. The effect of guanidinium was similar for M (Figure 4a) and Z (Figure 4b) antitrypsin. However, as inactivity may be due to loop–sheet polymerization as well as L-state formation, polymerization was also assessed over a range of guanidinium concentrations. In the absence of guanidinium neither M nor Z antitrypsin spontaneously polymerized on standing at 4 °C for 12 h. At 1.1 M guanidinium both M and Z antitrypsin had lost 60% inhibitory activity. In the case of Z antitrypsin this was all attributable to loop–sheet polymerization whereas

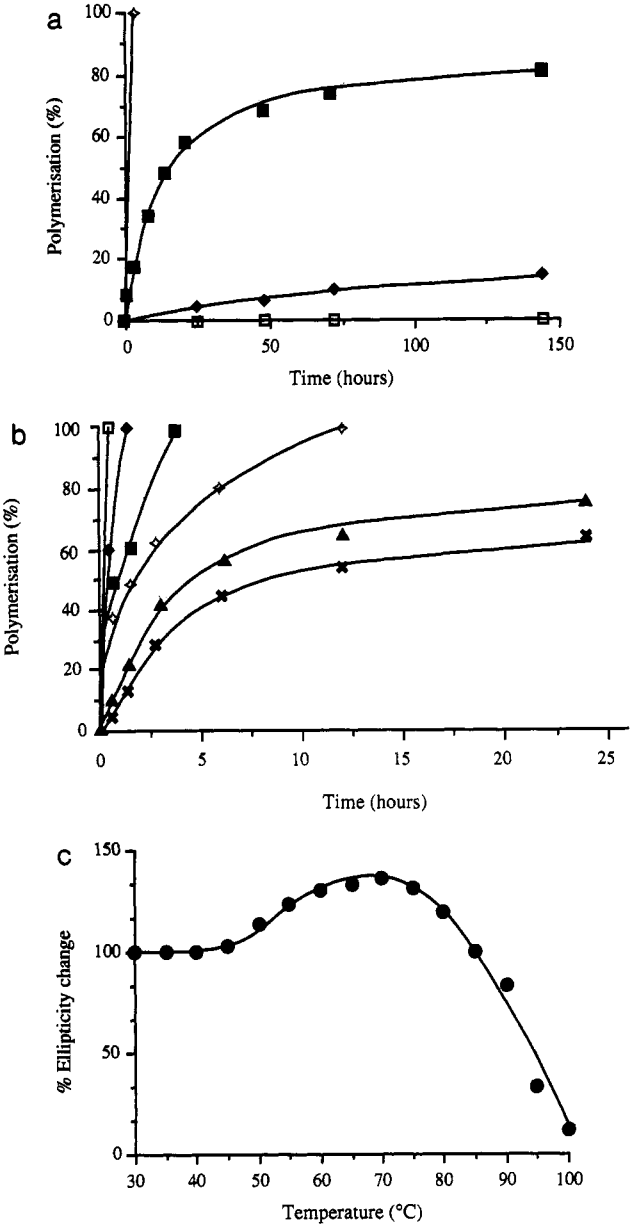

FIGURE 3: Effect of increasing temperature (a) and protein concentration (b) on the polymerization of M antitrypsin. The percentage polymerization at each time point was assessed by HPLC gel filtration using 10 μg of protein. Panel a was performed at 37 °C (⊡), 41 °C (♦), 50 °C (■), and 65 °C (four-pointed star) at a protein concentration of 2 mg/mL. The material incubated at 65 °C fully polymerized after 1-h incubation. Panel b was performed at 65 °C with a protein concentration of 1000 μg/mL (⊡), 500 μg/mL (♦), 250 μg/mL (■), 125 μg/mL (four-pointed star), 62.5 μg/mL (▲), and 31.25 μg/mL (×). Panel c shows the percentage change in ellipticity at 222 nm as compared to a native, unheated sample after incubating aliquots of M antitrypsin (0.2 mg/mL) at a range of temperatures for 3 h.

for M antitrypsin only 6% of the protein had polymerized. At 1.5 M guanidinium both M and Z antitrypsin had reached a plateau of inactivity; 65% and 29% of Z and M antitrypsin, respectively, had undergone loop–sheet polymerization. Thus although M and Z antitrypsin have similar inactivity profiles with guanidinium chloride, polymerization makes the largest contribution to this inactivity with Z antitrypsin and L-state formation to that of M antitrypsin.

Reversal of Polymerization with the Peptide BC13. Z antitrypsin (2 mg/mL) was polymerized by incubation at 37 °C for 4 days and then diluted with an equal volume of the free synthesized loop peptide BC13 so that the peptide was

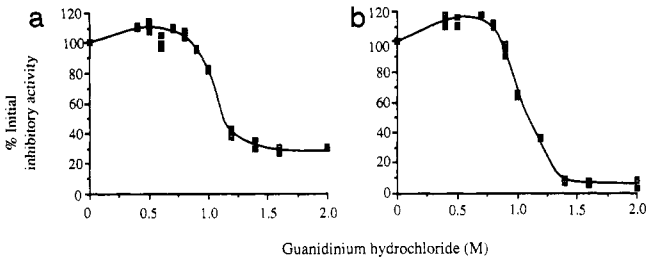

FIGURE 4: Inactivation of M (a) and Z (b) antitrypsin (1 mg/mL) after incubating with increasing concentrations of guanidinium chloride at 4 °C for 12 h. Following dilution with reaction buffer the residual inhibitory activity of both M and Z antitrypsin was determined against bovine α-chymotrypsin.

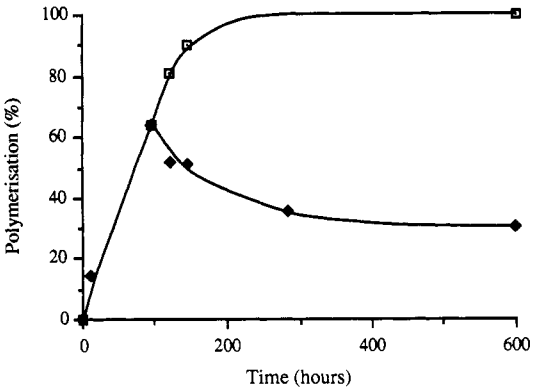

FIGURE 5: Effect of the reactive center loop peptide BC13 on the spontaneous polymerization of Z antitrypsin (2 mg/mL) at 37 °C. Z antitrypsin control (□), Z antitrypsin binary complex (♦) with the peptide added in 100-fold molar excess at 96 h. The percentage polymerization at each time point was assessed by HPLC gel filtration using 10 μg of protein.

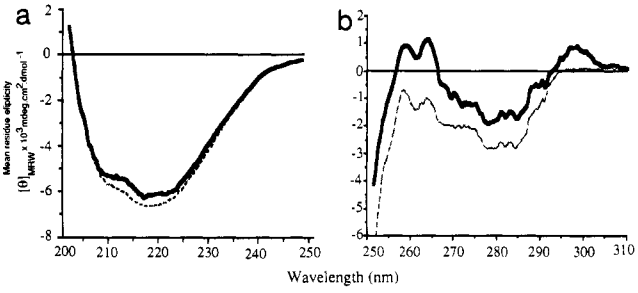

FIGURE 6: Circular dichroic spectra of M (bold line) and Z antitrypsin (pale line) at 0.1 mg/mL in the far- (100–250 nm) and near- (250–310 nm) UV range.

in 100-fold molar excess over the protein. A similar control sample was diluted with an equal volume of peptide buffer (50 mM Tris, 50 mM NaCl, pH 8.1, 10% acetonitrile). Antitrypsin diluted with buffer continued to polymerize whereas that diluted with peptide slowly dissociated to form a lower equilibrium position between the monomeric and polymeric forms (Figure 5). The same was apparent at 41 °C, but the rate at which the two forms reached equilibrium was reduced from 600 to approximately 150 h.

Circular Dichroism. Circular dichroic analysis (Figure 6) showed little difference between M and Z antitrypsin in the far-UV range (200–250 nm), indicating that the proteins share very similar secondary structures. A number of significant changes were apparent in the near-UV range (250–310 nm). The ^{342}Glu to Lys mutation of Z antitrypsin results in a reduction of ellipticity of the phenylalanine peaks at 256 and 264 nm, indicating a change in the environment of these residues. The trough at 280 nm which represents unresolved tryptophan and tyrosine residues also demonstrated more

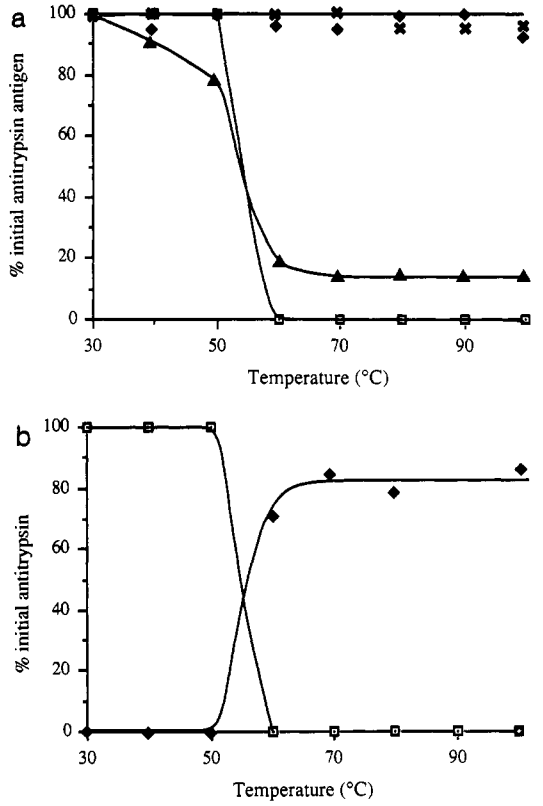

FIGURE 7: (a) *S* to *R* transition of M and Z antitrypsin (0.2 mg/mL). The *x*-axis is increasing temperature and the *y*-axis % of antigen remaining in solution measured against the value determined at 30 °C. Native M antitrypsin (□), cleaved M antitrypsin (♦), native Z antitrypsin (▲), cleaved Z antitrypsin (×). Panel b shows the effect of temperature on the heat stability (□) and loop–sheet polymerization (♦) of M antitrypsin (0.2 mg/mL).

negative ellipticity, whereas the peak at 295 nm was lost. This peak is due to either 194 or 238 tryptophan and indicates that one of these residues is in a less asymmetric environment.

The S to R Transition. Native and cleaved M antitrypsins (Figure 7a) had identical heat stability profiles to those described previously (Carrell & Owen, 1986). The profile for Z antitrypsin (Figure 7a) is similar, and the stability of the cleaved form confirms that Z antitrypsin undergoes the *S* to *R* transition. Intact Z antitrypsin precipitates at lower temperatures than M antitrypsin (<50 °C); despite this the point of inflection remains between 50 and 60 °C. Polymerization increased at the same point, as both M (Figure 7b) and Z antitrypsin (data not shown) precipitated, suggesting that loop–sheet polymerization and not denaturation and aggregation may account for the thermolability of these proteins. This was confirmed by subjecting the polymers to circular dichroic spectra examination at temperatures up to 100 °C. The polymers retained secondary structure following incubation for 2 h at temperatures up to 85 °C, but beyond this the material denatured. Thus the precipitation of antitrypsin at 56 °C results predominantly from loop–sheet polymerization.

Association Rate Constants and K_i Values for M and Z Antitrypsin. Previous SDS–PAGE analysis by Ogushi et al. (1987) suggested that the Z antitrypsin–neutrophil elastase complex was unstable. In order to confirm this, the association rate constant (k_{assn}) and K_i values of antitrypsin with elastase were determined. The K_i values for both M and Z antitrypsin were very low (<5 pM), indicating little complex dissociation and allowing the use of equations assuming the reaction to be irreversible. Using these equations, M and Z antitrypsin had

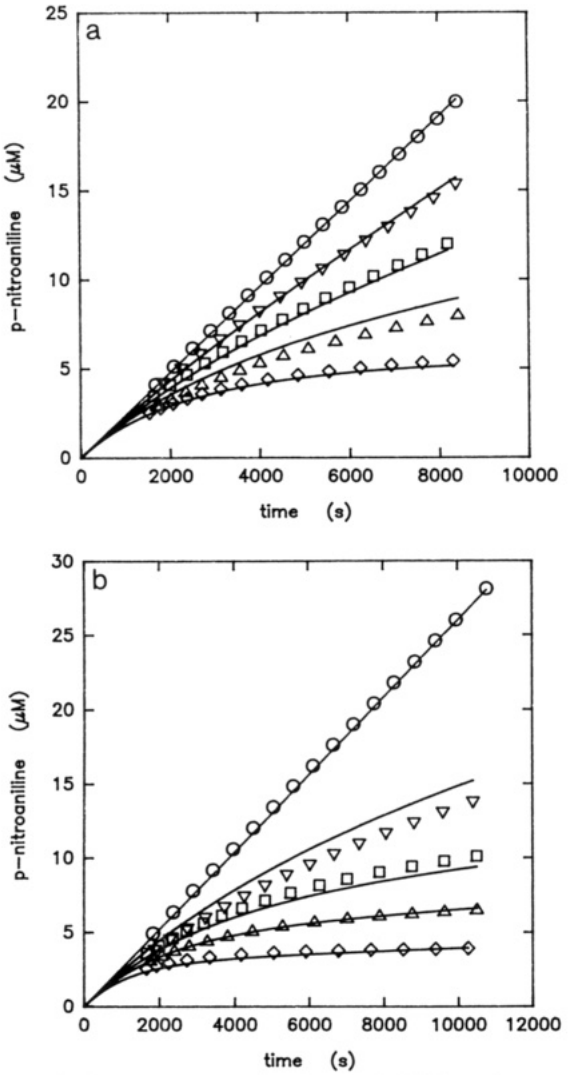

FIGURE 8: Progress curves showing the inhibition of neutrophil elastase by M (a) and Z (b) antitrypsin. The reaction in panel a was started with 56 pM elastase, and the curves represent 0, 18, 37, 55, and 92 pM M antitrypsin. The reaction in panel b was started with 56 pM elastase, and the curves represent 0, 94, 190, 280, and 470 pM Z antitrypsin. For the sake of clarity data points at less than 1500 s that were used in the regression analysis are not shown, and only each second point thereafter is shown. In addition, progress curves obtained at 74 pM M and 380 pM Z are not shown.

association rate constants with neutrophil elastase of (5.3 ± 0.06) × 10^7 and (1.2 ± 0.02) × 10^7 M^{-1} s^{-1}, respectively (Figure 8, panels a and b). The SDS–PAGE studies of Ogushi et al. (1987) were repeated with bovine α-chymotrypsin which like neutrophil elastase showed Z but not M antitrypsin–enzyme complex degradation (Figure 9); the predominant Z band having the mobility of reactive center cleaved, that is, post complex antitrypsin. Kinetic studies showed M and Z antitrypsin to have association rate constants with bovine α-chymotrypsin of (2.6 ± 0.2) × 10^6 and (2.2 ± 0.04) × 10^6 M^{-1} s^{-1}, respectively. The K_i values for both M and Z antitrypsin were low (9.2 ± 2.7 and 15 ± 4 pM, respectively), indicating tight complex formation with a complex half life of 8 and 4 h (M and Z antitrypsin, respectively).

Thus physiological complex dissociation does not account for the SDS–PAGE findings of Ogushi et al. (1987) for Z antitrypsin and elastase or our findings for Z antitrypsin with bovine α-chymotrypsin.

Cleavage of the Reactive Center Loop with Papaya Proteinase IV. Papaya proteinase IV is a Gly-specific cysteine

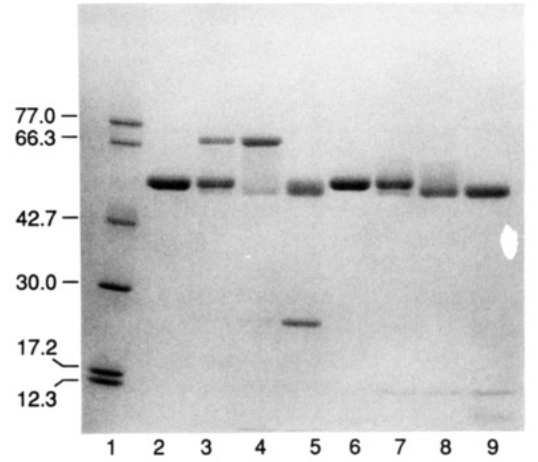

FIGURE 9: M and Z complex formation with bovine α-chymotrypsin. The enzyme and inhibitor were incubated together in 50% v/v reaction buffer for 30 min at room temperature before loading onto a 10–20% SDS–PAGE. All lanes contain 5 μg of protein. Lane 1, markers (kDa); lane 2, M antitrypsin; lane 3, M antitrypsin/chymotrypsin, ratio 1:0.5; lane 4, M antitrypsin/chymotrypsin, ratio 1:1; lane 5, M antitrypsin/chymotrypsin, ratio 1:2; lane 6, Z antitrypsin; lane 7, Z antitrypsin/chymotrypsin, ratio 1:0.5; lane 8, Z antitrypsin/chymotrypsin, ratio 1:1; lane 9, Z antitrypsin/chymotrypsin, ratio 1:2.

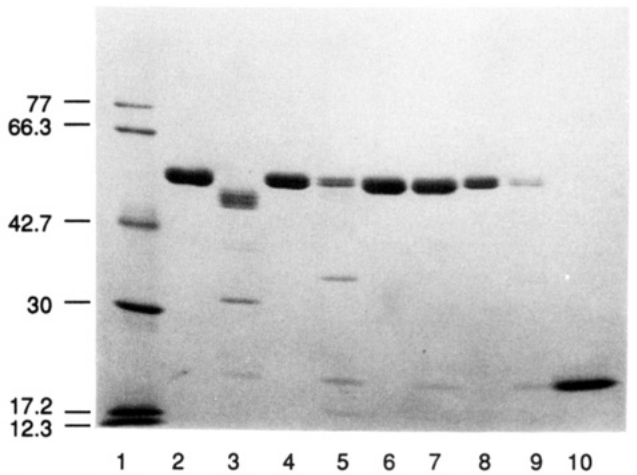

FIGURE 10: Cleavage of M and Z antitrypsin with papaya proteinase IV. M and Z binary complex were formed by incubation with the peptide BC13 for 24 h at 37 °C. Native or binary complexed M and Z antitrypsin were incubated in a 10:1 ratio with papaya proteinase IV in 50% v/v reaction buffer for 2 h at 37 °C before loading on a 10–20% SDS–PAGE. All lanes contain 5 μg of protein. Lane 1, markers (kDa); lane 2, M antitrypsin; lane 3, M antitrypsin + papaya proteinase IV; lane 4, Z antitrypsin; lane 5, Z antitrypsin + papaya proteinase IV; lane 6, M antitrypsin binary complex; lane 7, M binary complex + papaya proteinase IV; lane 8, Z antitrypsin binary complex; lane 9, Z binary complex + papaya proteinase IV; lane 10, papaya proteinase IV.

proteinase (Buttle et al., 1990) which cleaves M antitrypsin with one major product as shown in Figure 10 (lanes 2 and 3). Amino-terminal sequencing confirmed cleavage between residues P_9 and P_{10} of the reactive center loop in agreement with the findings of Mast et al. (1992). The major reactive center loop cleavage product was absent following the incubation of Z antitrypsin with papaya proteinase IV, indicating that the P_9–P_{10} bond was inaccessible in Z antitrypsin (lanes 4 and 5); indeed, the ^{342}Glu to Lys mutation completely distorted the cleavage profile of the antitrypsin molecule, producing a product compatible with cleavage at a site prior to and distant from the reactive center loop.

The binary complex of M antitrypsin with the peptide BC13 protected the reactive center loop from cleavage by papaya proteinase IV (lanes 6 and 7), but the same complex with Z

antitrypsin resulted in an identical cleavage pattern as the unmodified Z protein (lanes 8 and 9).

DISCUSSION

Purification of Z Antitrypsin. The Q-Sepharose elution profile (Figure 1) indicates that Z antitrypsin elutes at lower salt concentrations than M antitrypsin. This final step of the purification allows the separation of amino-terminally intact, normal-size (52-kDa) Z antitrypsin from both amino-terminally cleaved and intact high molecular weight material. The cleavage of 5 residues from the amino terminus results in the loss of 2 negatively charged amino acids and accounts for the early elution of this fraction from the anion-exchange column and its cathodal shift on isoelectric focusing (Figure 1, inset). The early eluting Z antitrypsin fractions had low specific activities and a significant high molecular weight contaminant. This may reflect antitrypsin denaturation and aggregation or loop–sheet polymerization (Lomas et al., 1992), which occurs spontaneously in the plasma of Z homozygotes (Cox et al., 1986). An alternative explanation is that this peak represents a high molecular weight contaminant not visualized by SDS–PAGE.

Loop–Sheet Polymerization of M and Z Antitrypsin. Z antitrypsin undergoes spontaneous loop–sheet polymerization at 37 °C, resulting in the loss of inhibitory activity against the proteinase bovine α-chymotrypsin (Figure 2). M, like Z antitrypsin, also undergoes loop–sheet polymerization but only at higher temperatures (Figure 3a). Thus there is no polymerization of M antitrypsin after 6 days of incubation at 37 °C, but slow polymerization does occur at 41 °C. Furthermore, as with Z antitrypsin (Lomas et al., 1992), the rate of polymerization is concentration dependent. The temperature of 65 °C was chosen to demonstrate this effect as at lower temperatures the relatively dilute solutions polymerize at much slower rates. Moreover, loop–sheet polymerization and not denaturation and aggregation account for the increase in molecular weight at temperatures up to 85 °C (Figure 3c). These observations account for the lack of polymerization seen in the plasma of M homozygotes (Cox et al., 1986) but also provide an explanation for the insoluble aggregates which are occasionally identified in the hepatocytes of healthy individuals. Antitrypsin is an acute-phase protein and as such undergoes a manifold increase in production in association with bouts of inflammation. The consequences of increased concentration (Figure 3b) coupled with the increase in temperature resulting from the inflammatory response may act to favor loop–sheet polymerization. The mechanism of such polymerization is identical to that described for Z antitrypsin (Lomas et al., 1992) in that it is blocked by peptide insertion and cleavage of the reactive center loop.

Interestingly, the rates of polymerization of M and Z antitrypsin following treatment with guanidinium chloride at 37 °C are similar, M antitrypsin reaching a higher proportion of polymerized material than Z. It appears that chaotropic agents such as extremes of temperature (beyond 60 °C) or mild denaturing conditions at 37 °C perturb the secondary structure to such an extent that they negate the effect of the ^{342}Glu to Lys mutation, and therefore under these conditions M and Z antitrypsin behave similarly. As expected, antitrypsin–BC13 binary complex formation blocked guanidinium-induced polymerization whereas a peptide that is unable to insert into the A-sheet of antitrypsin had little effect.

Antitrypsin, like other serpins, can be induced into the L-state by incubation in mild denaturing conditions for 12 h at 4 °C (Carrell et al., 1991). This process results from the insertion and locking of the reactive center loop into the A-sheet with the collapse of the optimal inhibtory structure, a conformation which accounts for the latent state of the serpin plasminogen activator inhibitor-1 (Mottonen et al., 1992). The collapse of the reactive center loop results in the loss of inhibitory activity as shown in Figure 4. However, the tendency for Z antitrypsin to polymerize is still apparent under conditions in which antitrypsin and other serpins (Carrell et al., 1991) form the L-state. Only if the guanidinium concentration is elevated beyond that required to produce maximum inhibition of antitrypsin activity does M antitrypsin show a significant degree of polymerization. Thus the local perturbation induced by the Z mutation favors the insertion of the reactive center loop of a second molecule rather than its own.

Attempts were made to reverse Z antitrypsin polymers formed by incubating the protein under physiological conditions. As with M antitrypsin (Evans, 1991) the addition of the peptide BC13 prevented further polymerization. Moreover, prolonged incubation over a period of 25 days at 37 °C resulted in a reduction in the amount of polymerized material from 64% to 31% (Figure 5). The same was true of incubation at 41 °C, but in this case the reduction occurred at a faster rate over a period of 6 days. Thus although reversal of polymerization can occur following incubation with a reactive loop peptide, it requires high concentrations and prolonged incubation preferably at raised temperatures. Furthermore, the monomeric antitrypsin liberated in this way is in the form of the binary complex and so will be inactive. Therefore, reactive loop peptides may have a role in preventing Z antitrypsin accumulation within the hepatocyte, but the prolonged incubation times and requirement for high concentrations reduce its value in the reversal of established polymers.

The S to R Transition. Native and cleaved M antitrypsins have identical heat stability profiles to those described previously (Carrell & Owen, 1986). The profile of Z antitrypsin is similar (Figure 7a), but the tendency to polymerize makes the curve slope downward between 30 and 50 °C; cleaved Z antitrypsin did not precipitate at temperatures up to 100 °C, confirming that the ^{342}Glu to Lys mutation does not affect the *S* to *R* transition. These findings confirm that cleavage of the reactive center loop of Z antitrypsin induces a conformational change in keeping with the circular dichroic spectra for native and cleaved antitrypsin reported previously (Lomas et al., 1992). Comparison between the Z antitrypin heat stability profile and the tendency to polymerize raised the suggestion that heat stability may be a measure of loop–sheet polymerization. This is borne out by Figure 7b, which shows M antitrypsin polymerization inversely paralleling heat-induced precipitation. Such loop–sheet polymerization occurs at temperatures up to 85 °C, beyond which the material loses secondary structure, indicating that denaturation and aggregation are then responsible for precipitation.

The sharp rise in polymerization between 50 and 60 °C for both M and Z antitrypsin accounts for the similar rates of polymerization at higher temperatures (Rowley et al., 1974). At this point the chaotropic effect of temperature is such that it drives the protein to polymerize irrespective of the ^{342}Glu to Lys mutation. Thus the change in thermal stability that is a feature of the *S* to *R* transition for serpins is a measure of the rate of protein polymerization and its prevention by the insertion of an extra strand into the A-sheet, whether by cleavage, peptide insertion, or L-state formation.

M and Z Antitrypsin Complex Stability. Ogushi et al. (1987) reported that immunopurified Z antitrypsin has a lower specific activity and lower association rate constant with neutrophil elastase than M antitrypsin. We found the specific activity of isolated unpolymerized Z and M antitrypsin to be similar (75% and 78%, respectively) but agree that the association rate constant of Z antitrypsin with neutrophil elastase was lower than that of M antitrypsin. However, the values reported here for both M and Z antitrypsin (Figure 8) are higher than those reported previously (Ogushi et al., 1987), with the value for M antitrypsin being closer to that of Beatty et al. (1980). Ogushi et al. (1987) also demonstrated that Z antitrypsin–neutrophil elastase complexes were unstable when assessed by SDS–PAGE. In order to clarify this, the K_i values of both M and Z antitrypsin with neutrophil elastase were determined. Somewhat surprisingly, these values were low, which indicated that the dissociation and degradation of the complex visualized by SDS–PAGE did not occur under physiological conditions. Indeed, the low K_i values suggest that complexes of both M and Z antitrypsin with neutrophil elastase have half-lives of 16 days.

These findings were repeated with bovine α-chymotrypsin. SDS–PAGE of M and Z antitrypsin complex formation confirmed the findings of Ogushi et al. (1987) with neutrophil elastase (Figure 9). Once again the Z antitrypsin–enzyme complex appeared to be unstable with degradation of the complex. The association rate constants for M and Z antitrypsin with bovine α-chymotrypsin were similar, and once against the K_i values suggested that the complexes should have half-lives of 8 and 4 h, respectively. Thus it appears that Z antitrypsin–enzyme complexes are stable under physiological conditions but are less resistant to treatment with SDS than M antitrypsin complexes.

The mild reduction in the association rate constant for Z antitrypsin with its cognate proteinase elastase indicates that the ^{342}Glu to Lys mutation has only a minor effect on the docking of enzyme and inhibitor, the initiating event in complex formation. The relative instability of these complexes following treatment with SDS suggests that the mutation prevents the locking of antitrypsin to the proteinase in order to form stable enzyme–inhibitor complexes.

Conformation of the Reactive Center Loop of Z Antitrypsin. The CD profiles (Figure 6) demonstrate the loss of the peak at 295 nm in Z antitrypsin, indicating perturbation in the environment of tryptophan 194 or 238. Such a change would result from a less asymmetric environment for either of these tryptophan residues. Structural modeling of antitrypsin crystal data shows that ^{194}Trp hydrogen bonds across the A-sheet to ^{341}Asp in M antitrypsin (Huber & Carrell, 1989; Schulze et al., 1990). Thus the Z mutation not only results in the breaking of the ^{342}Glu–^{290}Lys salt bridge (Loebermann et al., 1984) but also may allow the formation of a ^{342}Lys–^{341}Asp salt bridge which prevents ^{194}Trp–^{341}Asp hydrogen bond formation. The breaking of this bond is likely to induce dequenching of ^{194}Trp by placing the residue in a less asymmetric environment, but this change is insufficient to account for the gross changes in the phenylalanine and tyrosine contributions to the CD spectrum.

Qualitatively, the near-UV spectrum of Z antitrypsin is similar to that of M antitrypsin following partial insertion of an endogenous or exogenous peptide into the A-sheet. Such a profile may be achieved by either L-state or binary complex formation with a reactive center loop hexapeptide (Carrell et al., 1991). This would apparently imply that in Z antitrypsin the reactive center loop is overinserted into the A-sheet creating a near-UV CD profile similar to that of binary complexed M antitrypsin. The insertion could not be more than 1–2 residues as greater than that would induce changes in the secondary structure of antitrypsin and therefore alter the far-UV CD spectrum. Thus the ^{342}Glu to Lys mutation appears to open the gap in the A-sheet between strands 3 and 5, making the protein a receptor for the reactive center loop of a second antitrypsin molecule.

To assess whether the mutation at position 342 alters the accessibility of the reactive center loop, we used papaya proteinase IV which cleaves at the P_9–P_{10} bond. Structural models of antitrypsin have predicted that this bond lies outside the A-sheet (Carrell & Evans, 1992), and Mast et al. (1992) have shown it to be accessible to cleavage in M antitrypsin. The insertion of additional reactive center loop residues into the A-sheet would render this bond inaccessible to cleavage. Papaya proteinase IV was able to cleave M antitrypsin at the reactive center loop with a reduction of 4 kDa in the molecular mass (Figure 10). Z antitrypsin was not cleaved at this site, which is compatible with the insertion of 1–2 extra residues of the loop into the A-sheet. However, the cleavage of the reactive center loop of M antitrypsin by papaya proteinase IV is similarly blocked by the formation of the binary complex with the peptide BC13. This last finding is contrary to the results of Mast et al. (1992) who showed cleavage of the reactive center loop by papaya proteinase IV to be unaffected by the formation of the binary complex with a synthetic 16 mer reactive loop peptide. We hypothesize that during binary complex formation the inserted peptide expels the reactive center loop of M antitrypsin and forces it to adopt a helical conformation similar to that of ovalbumin. Such a conformation would place the P_9–P_{10} bond at the base of the final helical turn and so would prevent enzymatic cleavage. The discrepancy between our data and those of Mast et al. (1992) results from their lyophilization of the antitrypsin–peptide binary complex. This appears to open the reactive center loop, rendering it more accessible to proteolytic cleavage (unpublished observations). The binary complex of Z antitrypsin had a similar cleavage pattern to the native protein, suggesting that the reactive center loop of the native protein is expelled from the A-sheet into a binary complex-like helical conformation. Although there are conflicting results as to the conformation of the reactive center loop in Z antitrypsin, it is possible to conclude that the effect of the ^{342}Glu to Lys mutation is to open the A-sheet, allowing the Z antitrypsin molecule to act as a receptor for loop–sheet polymerization.

ACKNOWLEDGMENT

We thank Dr. L. C. Packman, Department of Biochemistry, University of Cambridge, for performing N-terminal sequencing.

REFERENCES

Baumann, U., Huber, R., Bode, W., Grosse, D., Lesjak, M., & Laurell, C. B. (1991) *J. Mol. Biol. 218*, 595–606.

Beatty, K., Bieth, J., & Travis, J. (1980) *J. Biol. Chem. 255*, 3931–3934.

Buttle, D. J., Ritonja, A., Pearl, L. H., Turk, V., & Barrett, A. J. (1990) *FEBS Lett. 260*, 195–197.

Carrell, R. W., & Owen, M. C. (1986) *Nature 322*, 730–732.

Carrell, R. W., & Evans, D. Ll. (1992) *Curr. Opin. Struct. Biol. 2*, 438–446.

Carrell, R. W., Evans, D. Ll., & Stein, P. E. (1991) *Nature 353*, 576–578.

Cox, D. W., Billingsley, G. D., & Callahan, J. W. (1986) *FEBS Lett. 205*, 255–260.

Evans, D. Ll. (1991) Thesis, University of Cambridge, U.K.
Evans, D. Ll., McGrogan, M., Scott, R. W., & Carrell, R. W. (1991) *J. Biol. Chem. 266*, 22307–22312.
Huber, R., & Carrell, R. W. (1989) *Biochemistry 28*, 8951–8966.
Jeppsson, J. O. (1976) *FEBS Lett. 65*, 195–197.
Kezdy, F. J., & Kaiser, E. T. (1970) *Methods Enzymol. 19*, 3–20.
Laemmli, U. K. (1970) *Nature 227*, 680–685.
Laurell, C. B., & Eriksson, S. (1963) *Scand. J. Clin. Lab. Invest. 15*, 132–140.
Laurell, C. B., Pierce, J., Persson, U., & Thulin, E. (1975) *Eur. J. Biochem. 57*, 107–113.
Loebermann, H., Tokuoka, R., Deisenhofer, J., & Huber, R. (1984) *J. Mol. Biol. 177*, 531–556.
Lomas, D. A., Evans, D. Ll., Finch, J., & Carrell, R. W. (1992) *Nature 357*, 605–607.
Mast, A. E., Enghild, J. J., & Salvesen, G. (1992) *Biochemistry 31*, 2720–2728.
Monte, M., Beuzard, Y., & Rosa, J. (1976) *Am. J. Clin. Pathol. 66*, 753–759.
Morrison, J. F., & Walsh, C. T. (1987) *Adv. Enzymol. Relat. Areas Mol. Biol. 61*, 201–301.
Mottonen, J., Strand, A., Symersky, J., Sweet, R. M., Danley, D. E., Geoghegan, K. F., Gerard, R. D., & Goldsmith, E. J. (1992) *Nature 355*, 270–273.
Ogushi, F., Fells, G. A., Hubbard, R. C., Straus, S. D., & Crystal, R. G. (1987) *J. Clin. Invest. 80*, 1366–1374.
Rowley, P. T., Sevilla, M. L., & Schwartz, R. H. (1974) *Biochem. Genet. 12*, 235–242.
Schulze, A. J., Baumann, U., Knof, S., Jaeger, E., Huber, R., & Laurell, C. B. (1990) *Eur. J. Biochem. 194*, 51–56.
Stein, P. E., Leslie, A. G. W., Finch, J. T., Turnell, W. G., McLaughlin, P. J., & Carrell, R. W. (1990) *Nature 347*, 99–102.
Stein, P. E., Leslie, A. G. W., Finch, J. T., & Carrell, R. W. (1991) *J. Mol. Biol. 221*, 941–959.
Stone, S. R., & Hofsteenge, J. (1986) *Biochemistry 25*, 4622–4628.
Towbin, H., Staehelin, T., & Gordon, J. (1979) *Proc. Natl. Acad. Sci. U.S.A. 76*, 4350–4354.
Travis, J., & Johnson, D. (1981) *Methods Enzymol. 80*, 754–765.
Weeke, B. (1973) *Scand. J. Immunol. 2* (Suppl. 1), 37–46.